About the simulation of primary grown-in microdefects in dislocation-free silicon single-crystal formation

V.I. Talanin, I.E. Talanin, and A.A. Voronin

Abstract: A mathematical model of primary grown-in microdefects formation is proposed. The model is built on the basis of the dissociative process of diffusion. Here, we study the interaction patterns between oxygen-vacancy (O + V) and carbon-interstitial (C + I) near the crystallization front in dislocation-free silicon monocrystals grown by float-zone and Czochralski methods. As shown here, the approximate analysis formulas obtained tally with the heterogeneous mechanism of grown-in microdefects formation.

PACS Nos.: 61.72Bb, 61.72.Jj, 61.72.Yx

Résumé : Nous proposons un modèle mathématique pour la formation des microdéfauts internes primaires. Le modèle se base sur le processus dissociatif de la diffusion. Nous étudions ici les patrons d'interaction entre une lacune d'oxygène (O + V) et le carbone interstitiel (C + I) près du front de cristalisation dans un monocristal de Si sans dislocation croissant par méthodes de flottaison ou de Czochralski. Comme nous le montrons ici, les formules approximatives d'analyse obtenues agréent avec le mécanisme hétérogène de formation des microdéfauts internes.

[Traduit par la Rédaction]

1. Introduction

Grown-in microdefects define not only the initial defect structure of dislocation-free silicon monocrystals, but further process-caused transformations of this structure as well. Hence, analysis of the grown-in microdefects-formation mechanism is a key to both solving the problem of defect structure control and to understanding the fundamental interaction of point defects.

Actually, there are two problem-solving approaches for grown-in microdefects formation. In the first-approach authors work within a point-defect dynamic model, where a crystal is taken as a dynamic system or a solid-state chemical reactor describing point-defect movement and interaction. Dynamic modelling of point defects is assumed to present a quantitative understanding of the grown-in microdefect formation process and the spatial distribution of the point defects [1–3]. This point-defect dynamics model covers convection, diffusion, and recombination of intrinsic point defects. Intrinsic point-defect fast recombination at near-melting-point temperature plays a crucial role in this model. It comes from

Received 10 September 2006. Accepted 29 March 2007. Published on the NRC Research Press Web site at http://cjp.nrc.ca/ on 17 November 2007.

V.I. Talanin,[1] I.E. Talanin, and A.A. Voronin. University of State and Municipal Government, Zhukovskii str. 70B, Zaporozhye 69002, Ukraine.

[1]Corresponding author (e-mail: v.i.talanin@mail.ru).

 doi: 10.1139/P07-094 © 2007 NRC Canada

the theoretical model of grown-in microdefects formation proposed by Voronkov that is a keystone of the point-defect dynamics model and its modifications [4]. Voronkov assumed the following: (*a*) the intrinsic point-defect recombination rate at a near-melting-point temperature is very high, (*b*) the diffusion factor of Si self-interstitials at near-melting-point temperature is higher than the diffusion factor of vacancies, (*c*) the vacancy equilibrium concentration at near-melting-point temperature is more than the equilibrium concentration of Si self-interstitials. The author showed that grown-in microdefects formation is controlled by $V/G = C_{\text{crit}}$ growth ratio (where V is a crystal growth rate and G is an axial temperature gradient). This theoretical model describes how vacancy microvoids (vacancies aggregates) are formed at $V/G > C_{\text{crit}}$ and how interstitial dislocation loops are formed at $V/G < C_{\text{crit}}$ in different crystal areas. From our point of view, notwithstanding the subsequent modification [5], an essential fault of Voronkov's model is that it does not properly account for interaction between intrinsic point defects and impurities.

The model of point-defect dynamics disregards such interaction as a whole [6]. It is implicitly presumed that during crystal cooling within the temperature range 1420 to 1150 °C the smallest (invisible) clusters of vacancies or Si self-interstitials are created. It is stated that at $T < 1150$ °C these clusters are transformed either into vacancy microvoids or interstitial dislocation loops according to ref. 6. Outside of the dynamics model, the "impurity – intrinsic point-defect" interaction, in particular for oxygen, may be taken into account only for crystals with high impurity content [7, 8].

The second approach relates to experimental investigations into the physical nature and characteristics of grown-in microdefects [9]. On the basis of these investigations, we built a qualitative heterogeneous mechanism of grown-in microdefects formation and transformation. Its keystones are as follows [10]:

- intrinsic point-defect recombination at near-melting-point temperature is insignificant due to the existence of a recombination barrier;
- cooling-induced decomposition of an intrinsic point-defect over-saturated solid solution at near-melting-point temperature follows two mechanisms: vacancy-type and interstitial-type;
- background impurities of oxygen and carbon are directly involved in the process of grown-in microdefects formation.

As is obvious, the principles of the heterogeneous formation mechanism are contrary to the theoretical principles used in Voronkov's model. Therefore, we believe that a lack of a relevant mathematical model is a central drawback of the heterogeneous mechanism.

The objective of this paper is to substantiate a theoretical model describing the heterogeneous formation mechanism for grown-in microdefects as a result of intrinsic point-defect – impurity interaction.

2. Physical model

We showed that oxygen-vacancy and carbon-interstitial agglomerates formed on impurity centers are drivers of the defect-formation process [10]. It is deduced from experiment that oxygen-vacancy and carbon-interstitial agglomerates ((I + V)-microdefects) start to form at near-melting-point temperatures [9]. As is well known, the vacancy microvoids and interstitial dislocation loops are induced by crystal cooling at temperatures below 1150 °C [6]. On the basis of the experimental results, we propose the concepts of primary grown-in microdefects ((I + V)-microdefects, D(C)-microdefects, B-microdefects), and secondary grown-in microdefects (A-microdefects, vacancy-type microvoids), which are based on the following interaction types: primary (fundamental) "impurity – intrinsic point defects", and secondary ("intrinsic point defects – intrinsic point defects"), according to ref. 10. Grown-in microdefects ranking (classification) was introduced by de Kock [11]. We have thoroughly analyzed it according to the new experimental results in ref. 10. In this paper, we reduce the range to two types of defects:

© 2007 NRC Canada

primary and secondary grown-in microdefects. First, this leads to the elimination of the confusion due to large-scale classification, and secondly, differences in the physics of primary and secondary grown-in defects formation are grounded.

From this, we suggest consideration of a crystal defect structure as a structure consisting of two subsystems: a subsystem of primary grown-in microdefects and a subsystem of secondary grown-in microdefects. The latter (vacancy microvoids and interstitial dislocation loops) may be described with Voronkov's theoretical model. This paper considers the formation process of primary grown-in microdefects, which is not described by the Voronkov model.

As noted above, intrinsic point defects formed in dislocation-free silicon monocrystals grown by float zone and Czochralski methods are recombined insignificantly near the crystallization front because of the occurrence of an entropy recombination barrier [9, 12]. As at near-melting-point temperatures, there are equilibrium concentrations of vacancies and silicon self-interstitials at the same time, the decomposition of point defects in an over-saturated solid-state solution follows two mechanisms simultaneously. According to the sign of the elastic crystal-lattice imperfections such mechanisms are either vacancy-type or interstitial-type [9]. Following the heterogeneous mechanism of grown-in microdefect formation, vacancies (V) and silicon self-interstitials (I) found drains as background oxygen (O) and carbon (C) impurities, respectively. At the initial phase of defect-formation these processes lead to the formation of vacancy-oxygen (V + O) and carbon-interstitial (C + I) complexes. Here, we can write the following quasi-chemical equations:

1. for the vacancy branch of the heterogeneous mechanism — $O_i + V \rightarrow (O + V)$
2. for the interstitial branch of the heterogeneous mechanism — $C_S + I \rightarrow (C + I)$,

where O_i represents oxygen interstitial atoms and C_S represents carbon atoms in a substituting position.

Such an idealized system is generic for undoped FZ–Si monocrystals vacuum-grown with oxygen and carbon impurities concentration of less than 5×10^{15} cm^{-3}. It should be noted that such a system does not account for the possible combined interaction between O_i and C_S. In addition, we should allow for other point defects (for example, iron, nitrogen, and doping impurities), which can exist and interact in industrially-grown FZ–Si and CZ–Si crystals.

This paper looks into an idealized system for four variables: vacancy, self-interstitials, oxygen, and carbon.

3. Mathematical model

We seek a solution within a model of impurities dissociative diffusion-migration [13]. The difference between this case and the decomposition phenomena is that, during the diffusion process, a dopant is entering the sample from an out-source and during decomposition a dopant is entering from inside the sample, i.e., lattice sites. In the both cases, the theoretical analysis is identical. But in a dissociative diffusion model, we should allow the impurity concentration to vary. This concentration decreases in the depth of the crystal with time and with coordinate x (where x is the length of crystal). The time constant is defined by the mechanism of migration within the sample and the dependence from a coordinate is defined by the shape of the sample and the boundary conditions of the diffusion problem.

It is complicated to interpret diffusion in multicomponent systems because the interaction of the impurity atoms should be taken into consideration. In the general case, a numerical computation is applied to the equations, subject only to certain assumptions, and we can obtain simple analytical formulas that can conveniently be compared with experiment. The complex-formation mechanism may vary, however, regardless of the nature of the driving forces leading to complex-formation. In our model, it is assumed that the range of driving is small. In this case, a complex may be taken as a point defect when analyzing point-defect migration.

© 2007 NRC Canada

Let us consider putting a complex formation as a quasi-chemical reaction

$$A + B \leftrightarrow AB \tag{1}$$

then the thermodynamic equilibrium condition between the free impurities A and B, and the impurity bound as a AB-complex may be written as

$$\mu_{\mathrm{A}} + \mu_{\mathrm{B}} = \mu_{\mathrm{AB}} \tag{2}$$

where μ_{A} and μ_{B} are the free impurity chemical potentials and μ_{AB} the complex's chemical potential.

If the total concentration of A and B impurities (N_{A} and N_{B}) is minor compared to the silicon atoms then in this approximation $\mu_{\mathrm{AB}} \approx \ln N_{\mathrm{AB}}$ and equilibrium condition (2) may be also written as

$$\frac{(N_{\mathrm{A}} - Q)(N_{\mathrm{B}} - Q)}{Q} = k(T) \tag{3}$$

where Q is the concentration of the complexes and $k(T)$ the temperature-dependent constant of the complex-formation reaction (at constant pressure) [13]. When $k = 0$, all impurities are bound in the complex (strong complex-formation).

It should be noted that in diffusion equations accounting for complex-formation, the total impurity flow consists of the free impurity flow and the complex-bound impurity flow [13]

$$\frac{\partial N_{\mathrm{A}}}{\partial t} = D_{\mathrm{A}} \frac{\partial^2 (N_{\mathrm{A}} - Q)}{\partial x^2} + D_Q \frac{\partial^2 Q}{\partial x^2} \tag{4}$$

$$\frac{\partial N_{\mathrm{B}}}{\partial t} = D_{\mathrm{B}} \frac{\partial^2 (N_{\mathrm{B}} - Q)}{\partial x^2} + D_Q \frac{\partial^2 Q}{\partial x^x} \tag{5}$$

where N_{A} and N_{B} are the impurity concentration and D_{A}, D_{B}, and D_Q are the diffusion coefficients of A- and B-component free complexes and the diffusion coefficient of the complexes, respectively.

The diffusion coefficient of the complexes depends on the complex-formation mechanism and on the component type that forms the complexes. In particular, if a complex is formed by two interacting atoms then the diffusion coefficient D_Q is much lower than the relevant atoms' diffusion coefficients (D_{A} and D_B). Therefore, considering complexes as slow-moving, we can neglect the last term members in (4) and (5).

$$\frac{\partial N_{\mathrm{A}}}{\partial t} = D_{\mathrm{A}} \frac{\partial^2 (N_{\mathrm{A}} - Q)}{\partial x^2} \tag{6}$$

$$\frac{\partial N_{\mathrm{B}}}{\partial t} = D_{\mathrm{B}} \frac{\partial^2 (N_{\mathrm{B}} - Q)}{\partial x^2} \tag{7}$$

Whereas complexes are immovable, boundary conditions are set for the free impurity. Since the time to come to equilibrium between the complexes and the free impurity is much less than the typical diffusion time then the total impurity concentration may be taken as an initial condition.

In ref. 13, a problem is considered for consecutive diffusion of component A in the sample, which is doped with component B, under initial and boundary conditions as follows:

$$N_{\mathrm{A}}(x,0) = 0, \qquad N_{\mathrm{B}}(x,0) = N_{\mathrm{B}}(\infty), \qquad N_{\mathrm{A}}(0,t) - Q(0,t) = H_{\mathrm{A}}(0)$$
$$\frac{\partial}{\partial x}\left[N_{\mathrm{B}}(x,t) - Q(x,t)\right]_{x=0} = 0 \tag{8}$$

© 2007 NRC Canada

Then, the diffusion equation solution is

$$\left.\begin{array}{l}\frac{1}{2}\left[N_{\mathrm{A}}-N_{\mathrm{B}}-k+\sqrt{k^2+2k\,(N_{\mathrm{A}}+N_{\mathrm{B}})+(N_{\mathrm{A}}-N_{\mathrm{B}})^2}\right]+2\lambda N'_{\mathrm{A}}=0\\ \frac{1}{2}\left[N_{\mathrm{B}}-N_{\mathrm{A}}-k+\sqrt{k^2+2k\,(N_{\mathrm{A}}+N_{\mathrm{B}})+(N_{\mathrm{A}}-N_{\mathrm{B}})^2}\right]+2\lambda d^2 N'_{\mathrm{B}}\end{array}\right\} \tag{9}$$

where $\lambda = x/2\sqrt{D_{\mathrm{A}} \times t}$ is a Boltzmann substitution, the prime denotes differentiation with respect to λ, $d^2 = D_{\mathrm{A}}/D_{\mathrm{B}}$ with D_{A} and D_{B} being the diffusion coefficient of the components.

A solution to system (9) with corresponding boundary conditions (an impurity diffusion from the constant source into the semiconductor uniformly doped with impurity B; impurity B is not evaporated) in case of strong complex-formation ($k = 0$) is [13]

$$N_{\mathrm{A}} = \begin{cases} N_{\mathrm{B1}} + H_{\mathrm{A}}(0)\left[1 - \frac{erf(\lambda/d_{\mathrm{A}})}{erf(\lambda_0/d_{\mathrm{A}})}\right], & \lambda < \lambda_0 \\ 0, & \lambda > \lambda_0 \end{cases} \tag{10}$$

$$N_{\mathrm{B}} = \begin{cases} N_{\mathrm{B1}}, & \lambda < \lambda_0 \\ N_{\mathrm{B0}}\left(1 - \frac{erfc(\lambda d)}{erfc(\lambda_0 d)}\right), & \lambda > \lambda_0 \end{cases} \tag{11}$$

where

$$N_{\mathrm{B1}} = \frac{N_{\mathrm{B0}}\,\mathrm{e}^{-\lambda_0 d^2}}{\sqrt{\pi}\lambda_0 d\, erfc(\lambda_0 d)} \tag{12}$$

while λ_0 is defined from the equation

$$\frac{\mathrm{e}^{\lambda_0^2(1-d^2)} erf(\lambda_0)}{erfc(\lambda_0 d)} = \frac{N_{\mathrm{A0}}}{N_{\mathrm{B0}}} \tag{13}$$

Let us rewrite the system (3)–(5) for diffusion impurity kinetics of mobile complexes in terms of total components $N_{\mathrm{A}} = H_{\mathrm{A}} + Q$ and $N_{\mathrm{B}} = H_{\mathrm{B}} + Q$

$$d_{\mathrm{A}}^2(N_{\mathrm{A}} - Q)'' + d_Q^2 Q'' + 2\lambda N'_{\mathrm{A}} = 0 \tag{14}$$

$$d_{\mathrm{B}}^2(N_{\mathrm{B}} - Q)'' + d_Q^2 Q'' + 2\lambda N'_{\mathrm{B}} = 0 \tag{15}$$

$$(N_{\mathrm{A}} - Q)(N_{\mathrm{B}} - Q) = k(T)Q \tag{16}$$

where $d_{\mathrm{A}}^2 = D_{\mathrm{A}}$, $d_{\mathrm{B}}^2 = D_{\mathrm{B}}$, and $d_Q^2 = D_Q$. D_Q is the complex diffusion coefficient, the prime denotes differentiation with respect to λ.

Note that in this case, a solution to the system of equations is considered for the three most commonly encountered cases in practice, namely, consecutive, simultaneous, and mutual diffusion. In our physical model environment, a consecutive diffusion may be considered when a no-flow condition is set for one of the components, which is in the volume of the sample at the reference time. In this case, the boundary conditions are as follows:

$$H_{\mathrm{A}}|_{\lambda=0} = H_{\mathrm{A}}(0), \quad H_{\mathrm{A}}|_{\lambda=\infty} = H_{\mathrm{A}}(\infty), \quad d_{\mathrm{B}}^2 H'_{\mathrm{B}} + d_Q^2\, Q'\big|_{\lambda=0} = 0, \quad H_{\mathrm{B}}|_{\lambda=\infty} = H_{\mathrm{B}}(\infty) \tag{17}$$

Generally, the system (14)–(16) with boundary conditions (17) has no analytical solutions, therefore, limiting cases must be considered to analyze the shape of the impurity profiles. Let us consider a strong complex-formation approximation ($k = 0$) that from physical view means that reaction $A + B \leftrightarrow Q$ is sharply offset to the complex-formation side. Furthermore, from the system (14)–(16) at $k = 0$, it formally follows that at least one free component concentration is zero, i.e., $H_{\mathrm{A}} = 0$ or $H_{\mathrm{B}} = 0$ (the impurity is completely bound to complexes).

© 2007 NRC Canada

A solution to the problem of component A diffusion into a semi-infinite sample, one-doped with component B subjected to no evaporation of component B from the sample and free component A available on the sample boundary is as follows [13]:

$$H_A = N_A - Q = \begin{cases} (N_A(0) - N_{B1})\left[1 - \frac{erfc(\lambda/d_A)}{erfc(\lambda_0/d_A)}\right], & \lambda \le \lambda_0 \\ 0, & \lambda > \lambda_0 \end{cases} \tag{18}$$

$$H_B = N_B - Q = \begin{cases} 0, & \lambda \le \lambda_0 \\ N_B(\infty)\left[1 - \frac{erfc(\lambda/d_B)}{erfc(\lambda_0/d_B)}\right], & \lambda > \lambda_0 \end{cases} \tag{19}$$

$$Q = \begin{cases} N_{B1}, & \lambda \ge \lambda_0 \\ N_{B1}\frac{erfc(\lambda/d_Q)}{erfc(\lambda_0/d_Q)}, & \lambda < \lambda_0 \end{cases} \tag{20}$$

$$\begin{aligned} N_{B1}S_1\left(\frac{\lambda_0}{d_Q}\right) &= N_B(\infty)S_1\left(\frac{\lambda_0}{d_B}\right) \\ N_{B1}S_1\left(\frac{\lambda_0}{d_Q}\right) &= \{N_A(0) - N_{B1}\}\,S_2\left(\frac{\lambda_0}{d_A}\right) \end{aligned} \tag{21}$$

where

$$S_1(x) = \frac{\exp(-x^2)}{\sqrt{\pi}x\,erfc(x)}, \qquad S_2(x) = \frac{\exp(-x^2)}{\sqrt{\pi}x\,erf(x)}, \qquad N_A(0) - N_{B1} = H_A(0)$$

4. Experimental

Within our physical model environment [9, 10], we take up component A as a background impurity (oxygen or carbon) and component B as intrinsic point defects (vacancies or self-interstitials). For the vacancy mechanism, we consider the oxygen + vacancy (O + V) interaction and for the interstitial mechanism we consider the carbon + self-interstitial (C + I) interaction. The following values are used in the calculations: $H_A(0) = H_o(0) = 4\times10^{15}$ cm^{-3} (FZ–Si), $H_A(0) = H_o(0) = 8\times10^{16}$ cm^{-3} (CZ–Si), $C_V = 8.84\times10^{14}$ cm^{-3}, $D_V = 4\times10^{-5}$ cm^2/s, $D_o = 0.17\exp(-2.54/kT)$, $k = 8.6153\times10^{-5}$ eV/K, $H_A(0) = H_c(T_m) = 4\times10^{15}$ cm^{-3} (FZ–Si), $H_A(0) = H_c(0) = 1\times10^{16}$ cm^{-3} (CZ–Si), $C_I(0) = 6.31\times10^{14}$ cm^{-3}, $D_I = 4.75\times10^{-4}$ cm^2/s, $D_c = 1.9\times\exp(-3.1/kT)$. A solution to (12) and (13) has a physical meaning ($N_{B1} \sim 10^{12}\ldots10^{14}$ cm^{-3}) only if $\lambda \approx 0.01$. It is worth noting that, in the approximation of strong complex-formation, λ_0 is interpreted as a complex-formation reaction-front boundary. Since x is a crystal length and the value $x = 0$ is the crystallization-front position, we can say that a complex-formation process takes place near the crystallization front.

These calculation data are confirmed by experimental investigations for initial phases of the defect-formation processes. They included the quenching of nondoped FZ–Si monocrystals 30 mm in diameter, which were vacuum-grown at varying growth rates (2.0, 3.0, 6.0, 9.0 mm/min). The most efficient crystal-quenching method was used, namely, decantation of a melted zone when at a given time this zone is short blown-off with a directed argon flow. The experiments allowed defining temperatures when grown-in microdefects are formed (Table 1) [9].

The quenching of FZ–Si crystals grown at $V = 6$ mm/min resulted in forming a so-called defect-free zone between the crystallization front and the area with D-microdefects available. Electron microscope investigations showed that the defect-free zone contained both interstitial and vacancy type defects sized 2 to 7 nm having concentration $\sim$4.5 $\times10^{13}$ cm^{-3} ((I + V)-microdefects) [9]. In FZ–Si crystals grown at $V = 9$ mm/min and subjected to quenching, interstitial and vacancy type defects were revealed in approximately comparable concentrations [9, 10].

© 2007 NRC Canada

Table 1. The formation temperatures of various microdefect types.

Growth rate (mm/min)	Growth conditions	Microdefects type	Length from crystallization front (mm)	Formation temperatures, ±20 K
2,0	Quenching	A	23	$T_A = 1373$
3,0	Quenching	B	—	$T_B = 1653$
6,0; 9,0	Quenching	I + V	—	$T_{I+V} = 1653$

Fig. 1. Curve family $T(x)$: (a) for FZ–Si crystals grown at $V = 1 \ldots 9.0$ mm/min, (b) for CZ–Si crystals grown at $V = 0.5 \ldots 3.0$ mm/min.

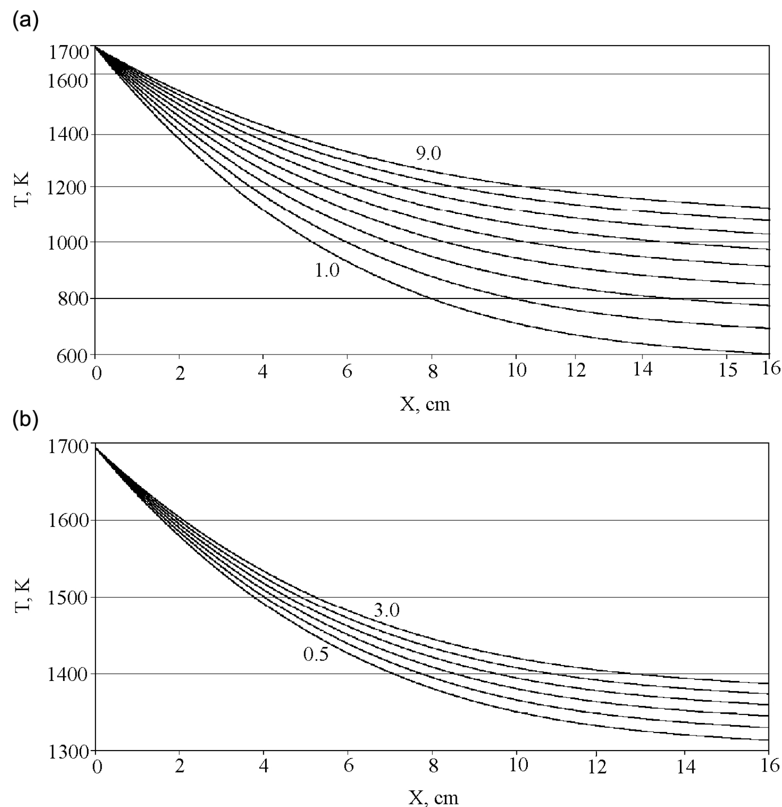

When investigating a separation surface, it was revealed that at a distance not more than 1–3 mm from the crystallization front dislocations were introduced on account of thermoshock. Hence, it was hard to determine exactly when the formation process of primary grown-in microdefects began. In view of this and based on the results shown in Table 1, we can conclude that primary grown-in microdefects are formed near the crystallization front [4].

Figures 1a and 1b display the $T(x)$ function for FZ–Si crystals (30 mm in diameter) and CZ–Si (50 mm in diameter). For FZ–Si crystals the $T(x)$ function is determined in accordance with empirical dependence [10]

$$\frac{dT}{dx} = 10 + (x - 16)^2 \exp(-61.2V - 0.28) \tag{22}$$

where x is the distance from the crystallization front to the section concerned, (cm) and V is crystal growth rate, (cm/s).

© 2007 NRC Canada

Fig. 2. Curve family (*a*) $C_V/C_V(0)$, (*b*) $C_{Q1}/C_{Q1}(0)$ as a function of the crystal length for CZ–Si.

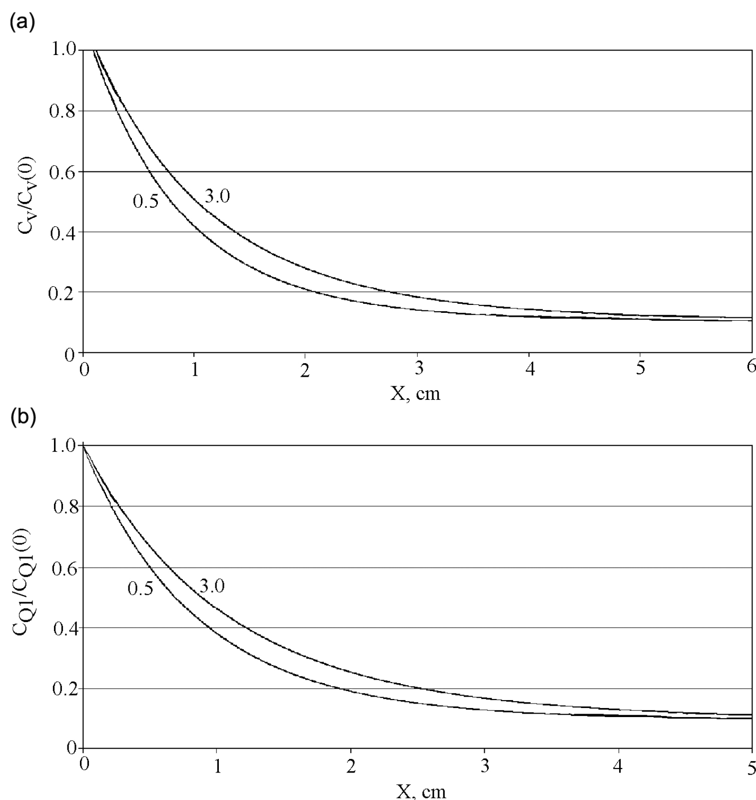

It was assumed for CZ–Si crystals that $G_{\mathrm{FZ-Si}} \approx 3G_{\mathrm{CZ-Si}}$, where G is the axial temperature gradient. Dependencies at $V = 1$ to 9.0 mm/min are provided for FZ–Si crystals and dependencies at $V = 0.5$ to 3.0 mm/min are provided for CZ–Si crystals. The radial temperature gradient is not taken into account and defect distribution is uniform along the crystal diameter.

Theoretical computations were carried out for vacancy (O + V) and interstitial (C + I) branches of the heterogeneous mechanism of grown-in microdefects formation in FZ–Si and CZ–Si crystals. Figures 2*a* and 2*b* display calculated graphical dependencies $C_V/C_V(0)$ and $C_{Q1}/C_{Q1}(0)$ as functions of CZ–Si crystal length within the range of growth rates 0.5 to 3.0 mm/min (where $C_V(0)$ and $C_{Q1}(0)$ are the concentration of vacancies and complexes (O + V) near the crystallization front).

Similarly, Figs. 3*a* and 3*b* display calculated graphic dependencies $C_I/C_I(0)$ and $C_{Q2}/C_{Q2}(0)$ as a functions of FZ–Si crystal length within a range of growth rates 1 to 9.0 mm/min (where $C_I(0)$ and $C_{Q2}(0)$ are the concentrations of silicon self-interstitials and (C + I) complexes near to the crystallization front). Indices 1 and 2 refer to vacancy and interstitial branches in the heterogeneous mechanism of grown-in microdefects, accordingly.

Analysis of the calculated curves' data shows a good match between the experimental data and the results of the grown-in microdefects heterogeneous formation mechanism. This refers to the temperatures of the primary grown-in microdefects formation and experiments in crystal quenching (Table 1), values of concentrations (I + V)-microdefects and D(C)-microdefects, defined by TEM-investigation results ($\sim 10^{13} \ldots 10^{14}$ cm^{-3}) [9, 10]. Therefore, notwithstanding the assumptions taken, it may be stated that the dissociative model of impurity diffusion is in good agreement with the experimental results obtained during the investigation of grown-in microdefects and, hence, may serve as a theoreti-

© 2007 NRC Canada

Fig. 3. Curve family (*a*) $C_I/C_I(0)$, (*b*) $C_{Q2}/C_{Q2}(0)$ as a function of the crystal length for FZ–Si.

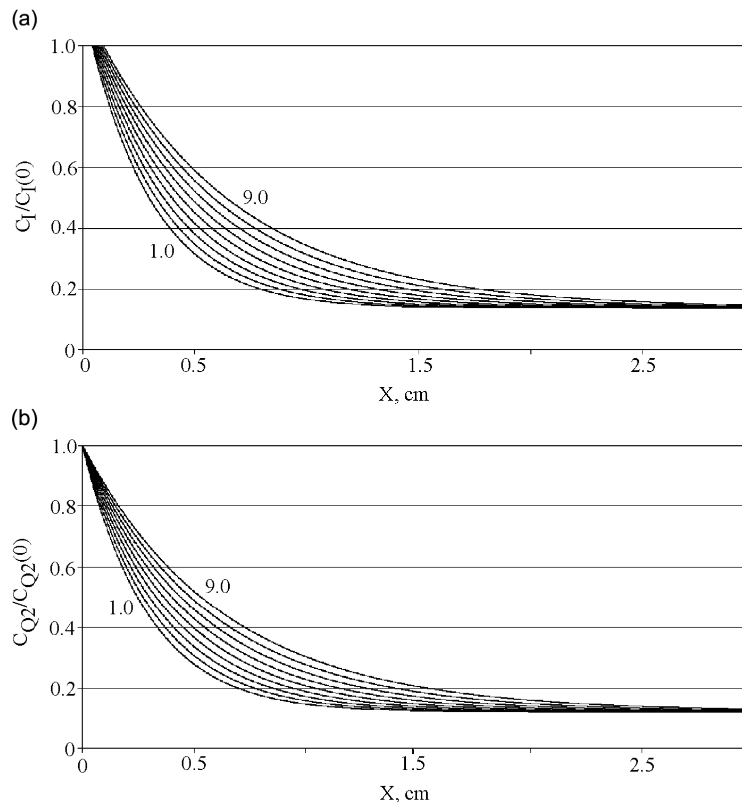

cal foundation to a heterogeneous mechanism of grown-in microdefect formation. Secondary grown-in microdefects (interstitial dislocation loops, vacancy microvoids) that occurred during crystal cooling below 1150 °C may be caused by both transformation of the initial defect structure of primary grown-in microdefects [9] and formation of the clusters of intrinsic point defects [10].

Thus, the qualitative heterogeneous model of grown-in microdefect formation that we proposed before [10] is presently based on the mathematical model that is created within the framework of dissociative diffusion theory. This approach is based on a fundamental interaction "impurity – intrinsic point defect". During crystal cooling within the temperature range 1420–1150 °C this interaction gives rise to the formation of primary grown-in microdefects, while the model of point-defect dynamics is based on "intrinsic point defect – intrinsic point defect" interaction [6]. Our model, as is shown in the Discussion, describes the formation of secondary grown-in microdefects when the crystal is cooled at temperatures below 1150 °C.

5. Discussion

As is well known, impurity atoms – intrinsic point defect interaction results in the formation of impurity centers and complexes [14–17]. They affect the electrical and physical properties of the semiconductor Si crucially [18].

However, the model of point-defect dynamics ignores the interaction between impurities and intrinsic point defects [1–3, 6–8]. It assumes a fast recombination of intrinsic point defects near the crystallization front [4, 6]. Depending on the V/G growth ratio the crystal has either vacancies only or Si self-

© 2007 NRC Canada

Fig. 4. Co-existence of vacancy (1) and interstitial (2) defects in CZ–Si.

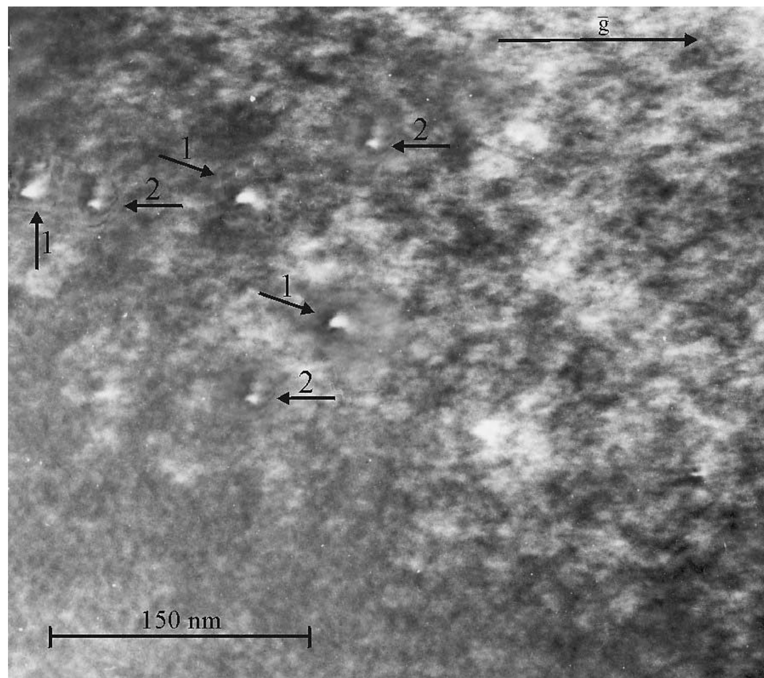

interstitials available. During crystal cooling below 1150 °C decomposition of the over-saturated solid-state solution of intrinsic point defects leads to homogeneous formation of vacancy microvoids and interstitial dislocation loops (A-microdefects), accordingly. Beyond the model of point-defect dynamics, it is assumed that impurity atoms may decorate vacancy microvoids (or interstitial dislocation loops) [7, 8]. Moreover, the V/G critical ratio dividing the interstitial zone (I-mode) and the vacancy zone (V-mode) of crystal growth may be influenced by doping [19]. The model of point-defect dynamics is based on experimental research for vacancy microviods and interstitial dislocation loops [20, 21].

However, the model of point-defect dynamics cannot explain the large amount of experimental research into the defect structure of dislocation-free Si monocrystals. There, analysis of impurities, which influence the formation of grown-in defects, proves that formation of A- and B-microdefects is intensified when the crystal is carbon-doped and hampered when the crystal is oxygen-doped [21, 22]. Local maxima of microdefect concentrations coincide with areas of phosphor in high concentration [23]. It is established that the presence of impurities (in particular, oxygen and carbon) is a key factor in the heterogeneous nature of grown-in microdefects formation [24–26]. It follows from experiment that oxygen and carbon play a dominant role in the formation of grown-in microdefects in large-scale CZ–Si monocrystals [27–30]. Oxygen concentration defines whether ordinary or double microvoids will be formed [20, 31]. Short-term thermal treatment ($t = 15 \ldots 30$ min, $T = 1100$ °C) causes a significant reduction in the dimensions of microvoids, causes changes in their structure, and also causes creation of large precipitates [20]. This experiment proves our assumption that vacancy microvoids are referred to secondary grown-in microdefects [10, 20].

Using transmission electronic microscopy, we showed the absence of intrinsic point-defect recombination near the crystallization front [9, 10]. We demonstrated that grown-in microdefects of both vacancy and interstitial type form and coexist [9, 10]. The problem of intrinsic point defects in a high temperature area is a keystone to understanding the mechanisms of defect formation in dislocation-free

© 2007 NRC Canada

Fig. 5. TEM-image of D-microdefects in interstitial growth mode ($V = 5$ mm/min, FZ–Si): 1 – vacancy defect; other defects are interstitial.

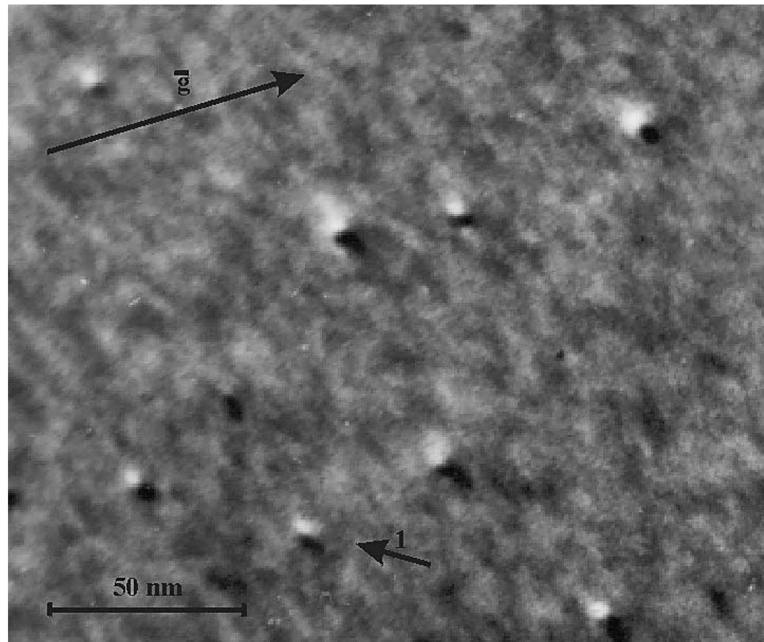

Si monocrystals. We proceeded with thermodynamical calculations to prove the experimental fact that recombination does not occur. We determined that the entropy recombination barrier is approximately equal to 2.1 eV [32]. Moreover, using three independent research methods (transmission electronic microscopy, diffuse X-ray scattering, and X-ray topography) it is established that vacancy-type grown-in D- and B-microdefects are formed in the interstitial growth mode of dislocation-free Si monocrystals [33]. Concentration of vacancy-type D- and B-microdefects is two orders lower than the concentration of interstitial-type D- and B-microdefects [33]. At the same time, the absence of A-microdefects in the same areas of crystal growth is indicative of heterogeneous mechanism of D- and B-microdefects formation. Figures 4 and 5 depict the results of our experimental research that support the theoretical calculations specified in this paper. We have already mentioned the detailed discussions for routine experiments and their results in refs. 9, 10, and 33, therefore, we omit these discussion here.

These experimental results disprove three fundamentals of Voronkov's theoretical model:

(1) recombination of intrinsic point defects near the crystallization front,

(2) a crystal growth area of one of either the vacancy-type or interstitial-type is available,and

(3) the formation mechanism of grown-in microdefects is homogeneous only.

Still, experimental research and Voronkov's theoretical model may be reconciled. This reconciliation follows from the real mechanism of defect formation in dislocation free Si monocrystals. That is to say, this mechanism includes two phases of defect formation. The first phase is heterogeneous (impurity – intrinsic point defect interaction). It is fundamental and leads to formation of primary grown-in microdefects ((I + V)-, D-, B-microdefects). This paper, for the first time, presents the mathematical model of primary grown-in microdefects formation. This model is meant for undoped dislocation-free FZ–Si and CZ–Si monocrystals and allows for four components: vacancies, intrinsic point defects,

© 2007 NRC Canada

carbon atoms, and oxygen atoms. The second phase is homogeneous. It is secondary (intrinsic point defect – intrinsic point defect interaction) and occurs at $T < 1150$ °C. This phase is accompanied by the formation of secondary grown-in microdefects (vacancy-type microvoids and A-microdefects). The model of point-defect dynamics (Voronkov's model) may serve as a mathematical model of secondary grown-in microdefects formation. If so, then Voronkov's model is a special case of a general model of grown-in microdefects formation. The general model of grown-in microdefects formation comprises both heterogeneous and homogeneous phases. Therefore, it is referred to as heterogeneous and diffusive.

6. Conclusion

The mathematical model of primary grown-in microdefects formation is formulated based on the dissociative diffusion process. Interaction patterns oxygen-vacancy (O + V) and carbon–silicon self-interstitial (C + I) have been examined near the crystallization front for dislocation-free silicon monocrystals grown by float-zone and Czochralski methods. Approximate analytical formulas are in good agreement with the heterogeneous mechanism of grow-in microdefects formation.

References

1. T. Sinno and R.A. Brown. J. Electrochem. Soc. **146**, 2300 (1999).
2. E. Dornberger, W. von Ammon, J. Virbulis, B. Hanna, and T. Sinno. J. Cryst. Growth, **230**, 291 (2001).
3. T. Sinno, R.A. Brown, W. von Ammon, and E. Dornberger. J. Electrochem. Soc. **145**, 302 (1998).
4. V.V. Voronkov. J. Cryst. Growth, **59**, 625 (1982).
5. V.V. Voronkov and R. Falster. J. Cryst. Growth, **194**, 76 (1998).
6. M.S. Kulkarni, V. Voronkov, and R. Falster. J. Electrochem. Soc. **151**, G663 (2004).
7. V.V. Voronkov and R. Falster. J. Electrochem. Soc. **149**, G167 (2002).
8. V.V. Voronkov and R. Falster. J. Appl. Phys. **91**, 5802 (2002) 5802.
9. V.I. Talanin and I.E. Talanin. *In* New research on semiconductors. *Edited by* T.B. Elliot. Nova Sci. Publications, New York. 2006. p. 35.
10. V.I. Talanin and I.E. Talanin. Defect & Diffusion Forum, **230–232**, 177 (2004).
11. A.J.R. de Kock. *In* Defects in semiconductors. North-Holland Publications Co., Amsterdam. 1981. p. 309.
12. U. Gosele, W. Frank, and A. Seeger. Solid State Commun. **45**, 31 (1983).
13. V.V. Vaskin and V.A. Uskov. Fizika Tverdogo Tela, **10**, 1239 (1968). (In Russian).
14. G.D. Watkins, J.R. Troxell, and A.P. Chatterjee. Defects and radiation effects in semiconductors. IOP, Bristol, London. 1979. Vol. 46. p. 16.
15. A. Bourret, J. Thibault-Desseaux, and D.N. Seidman. J. Appl. Phys. **55**, 825 (1984).
16. J. Leroueille. Phys. Status Solidi, **74**, K159 (1982).
17. L.F. Makarenko. Physica B, **465**, 308 (2001).
18. G.A. Rozgonyi. Solid State Technol. **19**, 49 (1976).
19. M. Porrini, V.V. Voronkov, and R. Falster. Mater. Sci. Eng. B, **134**, 185 (2006).
20. M. Itsumi. J. Cryst. Growth, **1773**, 237 (2002).
21. H. Foll, V. Gosele, and B.O. Kolbesen. J. Cryst. Growth, **40**, 90 (1977).
22. T. Abe, H. Harada, and J. Chikawa. Physica BC, **116**, 139 (1983).
23. J.B. Kamm and R. Muller. Sol. State Electr. **20**, 105 (1977).
24. B.O. Kolbesen and A. Muhlbauer. Sol. State Electr. **25**, 1561 (1977).
25. K.V. Ravi. Imperfections and impurities in semiconductor silicon. Wiley, New York. 1981. 470 p.
26. P.J. Drevinsky, C.E. Caefer, L.C. Kimerling, and J.L. Benton. Defect control in semiconductors. Elsevier, Amsterdam. 1990. Vol. 1. p. 341.
27. M. Ogino. Appl. Phys. Lett. **41**, 847 (1983).
28. T. Ueki, M. Itsumi, and T. Takeda. Jpn. J. Appl. Phys. **38**, 5695 (1999).
29. K. Kim Young, S. Ha Tae, and J.K. Yoon. J. Mater. Sci. **33**, 4627 (1998).
30. S. Iida, Y. Aoki, Y. Sugita, T. Abe, and H. Kawata. Jpn. J. Appl. Phys. **39**, 6130 (2000).

© 2007 NRC Canada

31. T. Ueki, M. Itsumi, T. Takeda, K. Yoshida, A. Takaoka, and S. Nakajima. Jpn. J. Appl. Phys. **37**, L771 (1998).
32. V.I. Talanin and I.E. Talanin. Phys. Solid State, **49**, 467 (2007).
33. V.I. Talanin and I.E. Talanin. Ukr. J. Phys. **51**, 1109 (2006).

© 2007 NRC Canada